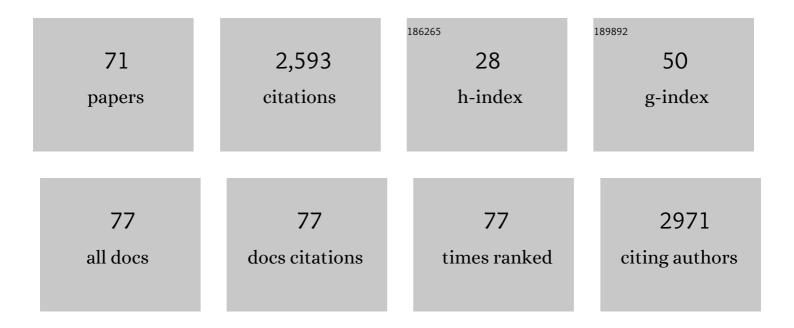
List of Publications by Year in descending order

Source: https://exaly.com/author-pdf/6756648/publications.pdf Version: 2024-02-01



#	Article	IF	CITATIONS
1	Conformational Adaptation of βâ€Peptide Foldamers for the Formation of Metal–Peptide Frameworks. Angewandte Chemie - International Edition, 2022, 61, .	13.8	14
2	Conformational Adaptation of βâ€₽eptide Foldamers for the Formation of Metal–Peptide Frameworks. Angewandte Chemie, 2022, 134, .	2.0	5
3	Reductive Carbonylation of Nitroarenes Using a Heterogenized Phen-Pd Catalyst. Inorganic Chemistry, 2022, 61, 1552-1561.	4.0	5
4	Nickel-Catalyzed NO Group Transfer Coupled with NO _{<i>x</i>} Conversion. Journal of the American Chemical Society, 2022, 144, 4585-4593.	13.7	6
5	Frontispiz: Conformational Adaptation of βâ€Peptide Foldamers for the Formation of Metal–Peptide Frameworks. Angewandte Chemie, 2022, 134, .	2.0	0
6	Binding of carbon monoxide at a single nickel center and its oxidative reactivity toward <scp>CO₂</scp> and <scp>O₂</scp> . Bulletin of the Korean Chemical Society, 2022, 43, 222-226.	1.9	1
7	Frontispiece: Conformational Adaptation of βâ€Peptide Foldamers for the Formation of Metal–Peptide Frameworks. Angewandte Chemie - International Edition, 2022, 61, .	13.8	2
8	Chemoselective hydrogenation of α,β-unsaturated carbonyl compounds using a recyclable Ru catalyst embedded on a bisphosphine based POP. Journal of Industrial and Engineering Chemistry, 2021, 94, 361-367.	5.8	7
9	Ni(0)-promoted activation of C _{sp2} –H and C _{sp2} –O bonds. Chemical Science, 2021, 12, 9983-9990.	7.4	3
10	Metal–ligand cooperative transformation of alkyl azide to isocyanate occurring at a Co–Si moiety. Chemical Communications, 2021, 57, 3219-3222.	4.1	8
11	Axial Redox Tuning at a Tetragonal Cobalt Center. Inorganic Chemistry, 2021, 60, 5647-5659.	4.0	2
12	Rapid ignition of "green―bipropellants enlisting hypergolic copper (II) promoter-in-fuel. Fuel, 2021, 297, 120734.	6.4	16
13	Metal–ligand cooperativity of a Co–P moiety. Inorganic Chemistry Frontiers, 2020, 7, 1172-1181.	6.0	6
14	Photophysical Tuning of σ-SiH Copper-Carbazolide Complexes To Give Deep-Blue Emission. Inorganic Chemistry, 2020, 59, 315-324.	4.0	7
15	Metal-Ligand Cooperativity of Phosphorus-Containing Pincer Systems. Topics in Organometallic Chemistry, 2020, , 71.	0.7	0
16	Divergent Strategies for the π-Extension of Heteroaryl Halides Using Norbornadiene as an Acetylene Synthon. Organic Letters, 2020, 22, 9670-9676.	4.6	12
17	Additive-promoted hypergolic ignition of ionic liquid with hydrogen peroxide. Combustion and Flame, 2020, 214, 426-436.	5.2	39
18	Catalytic hydrogenation of CO ₂ at a structurally rigidified cobalt center. Inorganic Chemistry Frontiers, 2020, 7, 1845-1850.	6.0	6

#	Article	IF	CITATIONS
19	A Silyl-Nickel Moiety as a Metal–Ligand Cooperative Site. Inorganic Chemistry, 2019, 58, 11534-11545.	4.0	17
20	A Lowâ€Spin Threeâ€Coordinate Cobalt(I) Complex and Its Reactivity toward H ₂ and Silane. Angewandte Chemie - International Edition, 2019, 58, 6938-6942.	13.8	26
21	A Lowâ€Spin Threeâ€Coordinate Cobalt(I) Complex and Its Reactivity toward H 2 and Silane. Angewandte Chemie, 2019, 131, 7012-7016.	2.0	10
22	One metal is enough: a nickel complex reduces nitrate anions to nitrogen gas. Chemical Science, 2019, 10, 4767-4774.	7.4	33
23	Anionic Doping and Cationic Site Preference in CaYb ₄ Al ₂ Sb _{6–<i>x</i>} Ge _{<i>x</i>} (<i>x</i> = 0.2, 0.5,) Tj Chemistry, 2019, 58, 5827-5836.	ETQ ₈ 11	0.784314 rgi
24	Enhancing Trust of Supply Chain Using Blockchain Platform with Robust Data Model and Verification Mechanisms. , 2019, , .		7
25	Selective Transformation of CO ₂ to CO at a Single Nickel Center. Accounts of Chemical Research, 2018, 51, 1144-1152.	15.6	43
26	Designing Redox‧table Cobalt–Polypyridyl Complexes for Redox Flow Batteries: Spin rossover Delocalizes Excess Charge. Advanced Energy Materials, 2018, 8, 1702897.	19.5	38
27	Direct CO ₂ Addition to a Ni(0)–CO Species Allows the Selective Generation of a Nickel(II) Carboxylate with Expulsion of CO. Journal of the American Chemical Society, 2018, 140, 2179-2185.	13.7	52
28	Enhanced Doubly Activated Dual Emission Fluorescent Probes for Selective Imaging of Glutathione or Cysteine in Living Systems. Analytical Chemistry, 2018, 90, 2648-2654.	6.5	137
29	HERMES: GS1-based Smart City Service Intercommunity. , 2018, , .		2
30	A Pâ^'P Bond as a Redox Reservoir and an Active Reaction Site. Angewandte Chemie, 2018, 130, 14355-14359.	2.0	3
31	Poly(amide-imide) materials for transparent and flexible displays. Science Advances, 2018, 4, eaau1956.	10.3	57
32	A Pâ^'P Bond as a Redox Reservoir and an Active Reaction Site. Angewandte Chemie - International Edition, 2018, 57, 14159-14163.	13.8	17
33	Bond Rotation in an Aromatic Carbaporphyrin: Allyliporphyrin. Chemistry - A European Journal, 2018, 24, 10054-10058.	3.3	10
34	Well-Defined Cesium Benzotriazolide as an Active Catalyst for Generating Disubstituted Ureas from Carbon Dioxide and Amines. ChemCatChem, 2017, 9, 215-216.	3.7	0
35	Novel intramolecular ï€â€"΀-interaction in a BODIPY system by oxidation of a single selenium center: geometrical stamping and spectroscopic and spectrometric distinctions. Dalton Transactions, 2017, 46, 4111-4117.	3.3	16
36	Ïf-Complexation as a strategy for designing copper-based light emitters. Chemical Communications, 2017, 53, 2858-2861.	4.1	31

#	Article	IF	CITATIONS
37	A Tâ€Shaped Nickel(I) Metalloradical Species. Angewandte Chemie, 2017, 129, 9630-9634.	2.0	28
38	A Tâ€Shaped Nickel(I) Metalloradical Species. Angewandte Chemie - International Edition, 2017, 56, 9502-9506.	13.8	75
39	Computer-aided rational design of Fe(<scp>iii</scp>)-catalysts for the selective formation of cyclic carbonates from CO ₂ and internal epoxides. Catalysis Science and Technology, 2017, 7, 4375-4387.	4.1	34
40	Single and double-doping effects on the thermoelectric properties of two Zintl compounds: Eu ₁₁ Bi _{8.07(2)} Sn _{1.93} and Eu _{10.74(2)} K _{0.26} Bi _{9.14(2)} Sn _{0.86} . Dalton Transactions, 2017, 46, 11840-11850.	3.3	10
41	Rücktitelbild: A Tâ€Shaped Nickel(I) Metalloradical Species (Angew. Chem. 32/2017). Angewandte Chemie, 2017, 129, 9754-9754.	2.0	Ο
42	Wellâ€Đefined Cesium Benzotriazolide as an Active Catalyst for Generating Disubstituted Ureas from Carbon Dioxide and Amines. ChemCatChem, 2017, 9, 247-252.	3.7	13
43	Carbon dioxide binding at a Ni/Fe center: synthesis and characterization of Ni(η ¹ -CO ₂ -κC) and Ni-ι⁄4-CO ₂ -κC:κ ² O,O′-Fe. Chemical S 2017, 8, 600-605.	cien≄e,	44
44	Synthesis and characterization of a four-coordinate nickel carbamato species (MeSiP i Pr 2) Tj ETQq0 0 0 rgBT /C Chimica Acta, 2017, 460, 55-62.	verlock 10 2.4	0 Tf 50 467 To 11
45	The unusual hydridicity of a cobalt bound Si–H moiety. Chemical Communications, 2016, 52, 9367-9370.	4.1	18
46	Alkoxide Migration at a Nickel(II) Center Induced by a π-Acidic Ligand: Migratory Insertion versus Metal–Ligand Cooperation. Inorganic Chemistry, 2016, 55, 12863-12871.	4.0	28
47	Formation of a tetranickel octacarbonyl cluster from the CO ₂ reaction of a zero-valent nickel monocarbonyl species. Inorganic Chemistry Frontiers, 2016, 3, 849-855.	6.0	21
48	Reversible Intramolecular P–S Bond Formation Coupled with a Ni(O)/Ni(II) Redox Process. Organometallics, 2016, 35, 1586-1592.	2.3	20
49	Foldecture as a Core Material with Anisotropic Surface Characteristics. Journal of the American Chemical Society, 2015, 137, 2159-2162.	13.7	32
50	Crystal Structure, Chemical Bonding and Magnetism Studies for Three Quinary Polar Intermetallic Compounds in the (Eu1â^'xCax)9In8(Ge1â^'ySny)8 (x = 0.66, y = 0.03) and the (Eu1â^'xCax)3In(Ge3â^'ySn1+y) (x <i>=</i> }.1j ET(QqQOOrgBT/
51	Phosphinite-Ni(0) Mediated Formation of a Phosphide-Ni(II)-OCOOMe Species via Uncommon Metal–Ligand Cooperation. Journal of the American Chemical Society, 2015, 137, 4280-4283.	13.7	58
52	Mechanistic Study on C–C Bond Formation of a Nickel(I) Monocarbonyl Species with Alkyl Iodides: Experimental and Computational Investigations. Organometallics, 2015, 34, 4305-4311.	2.3	25
53	Vanadyl–Catecholamine Hydrogels Inspired by Ascidians and Mussels. Chemistry of Materials, 2015, 27, 105-111.	6.7	61
54	Efficient Synthesis of Frutinoneâ€A and Its Derivatives through Palladium atalyzed CH Activation/Carbonylation. Chemistry - an Asian Journal, 2015, 10, 878-881.	3.3	25

#	Article	IF	CITATIONS
55	Hydrogen-Bond-Assisted Controlled C–H Functionalization via Adaptive Recognition of a Purine Directing Group. Journal of the American Chemical Society, 2014, 136, 1132-1140.	13.7	146
56	Facile <i>meso</i> -BODIPY Annulation and Selective Sensing of Hypochlorite in Water. Organic Letters, 2014, 16, 520-523.	4.6	156
57	Transmethylation of a four-coordinate nickel(<scp>i</scp>) monocarbonyl species with methyl iodide. Chemical Science, 2014, 5, 3853-3858.	7.4	49
58	Single-Crystal Growth and Size Control of Three Novel Polar Intermetallics: Eu _{2.94(2)} Ca _{6.06} In ₈ Ge ₈ , Eu _{3.13(2)} Ca _{5.87} In ₈ Ge ₈ , and Sr _{3.23(3)} Ca _{5.77} In ₈ Ge ₈ with Crystal Structure, Chemical Bonding, and Magnetism Studies. Inorganic Chemistry, 2014, 53, 4669-4677.	4.0	8
59	Formation of a nickel carbon dioxide adduct and its transformation mediated by a Lewis acid. Chemical Communications, 2014, 50, 11458-11461.	4.1	74
60	Heterolytic H ₂ Cleavage and Catalytic Hydrogenation by an Iron Metallaboratrane. Organometallics, 2013, 32, 3053-3062.	2.3	199
61	Synthesis and Reactivity of Nickel(II) Hydroxycarbonyl Species, NiCOOH-κ <i>C</i> . Organometallics, 2013, 32, 7195-7203.	2.3	61
62	Silylation of Iron-Bound Carbon Monoxide Affords a Terminal Fe Carbyne. Journal of the American Chemical Society, 2011, 133, 4438-4446.	13.7	76
63	A Nonclassical Dihydrogen Adduct of <i>S</i> = ¹ / ₂ Fe(I). Journal of the American Chemical Society, 2011, 133, 16366-16369.	13.7	59
64	Triggering N2 uptake via redox-induced expulsion of coordinated NH3 and N2 silylation at trigonal bipyramidal iron. Nature Chemistry, 2010, 2, 558-565.	13.6	285
65	Sulfur Donor Atom Effects on Copper(I)/O ₂ Chemistry with Thioanisole Containing Tetradentate N ₃ S Ligand Leading to μ-1,2-Peroxo-Dicopper(II) Species. Inorganic Chemistry, 2010, 49, 8873-8885.	4.0	37
66	Thioether S-ligation in a side-on μ-η ² :η2-peroxodicopper(ii) complex. Chemical Communications, 2010, 46, 91-93.	4.1	29
67	Copper(I)/O ₂ Chemistry with Imidazole Containing Tripodal Tetradentate Ligands Leading to 1¼-1,2-Peroxoâ^'Dicopper(II) Species. Inorganic Chemistry, 2009, 48, 11297-11309.	4.0	47
68	Dinitrogen Complexes Supported by Tris(phosphino)silyl Ligands. Inorganic Chemistry, 2009, 48, 2507-2517.	4.0	139
69	Thiol-copper(I) and disulfide–dicopper(I) complex O2-reactivity leading to sulfonate–copper(II) complex or the formation of a cross-linked thioether–phenol product with phenol addition. Journal of Inorganic Biochemistry, 2007, 101, 1845-1858.	3.5	16
70	Thioether Sulfur Oxygenation from O2 or H2O2 Reactivity of Copper Complexes with Tridentate N2Sthioether Ligands. Inorganic Chemistry, 2006, 45, 10098-10107.	4.0	36
71	A molecular pinwheel multicopper(i) cluster, [(LSâ^')6Cul13(S2â^')2]3+with μ4-sulfido, μ3-thiolato and nitrogenligands. Chemical Communications, 2006, , 621-623.	4.1	25